Accepted Manuscript

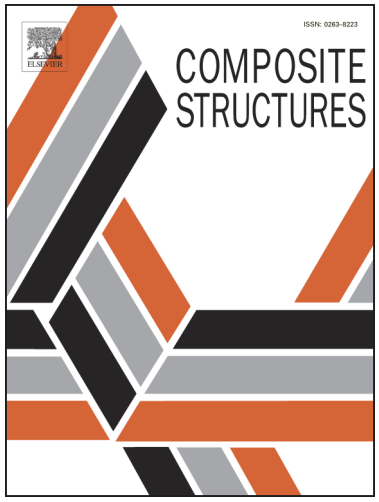

An Experimental Study of Scaling Effects in the Perforation Resistance of Woven CFRP Laminates

Z.W. Xu, Z.W. Guan, W.J. Cantwell

PII: S0263-8223(17)31543-X
DOI: http://dx.doi.org/10.1016/j.compstruct.2017.08.077
Reference: COST 8835

To appear in: *Composite Structures*

Received Date: 28 April 2017
Revised Date: 14 July 2017
Accepted Date: 18 August 2017

Please cite this article as: Xu, Z.W., Guan, Z.W., Cantwell, W.J., An Experimental Study of Scaling Effects in the Perforation Resistance of Woven CFRP Laminates, *Composite Structures* (2017), doi: http://dx.doi.org/10.1016/j.compstruct.2017.08.077

An Experimental Study of Scaling Effects in the Perforation Resistance of Woven CFRP Laminates

Z.W. Xu[1], Z.W. Guan[1,2] and W.J. Cantwell[3]

[1] School of Engineering, University of Liverpool, Liverpool L69 3GH, UK.

[2]School of Mechanical Engineering, Chengdu University, Shiling Town, Chengdu City, Sichuan, China.

[3] Department of Aerospace Engineering, Khalifa University of Science and Technology, Abu Dhabi, United Arab Emirates.

Abstract

Scaling effects in the perforation resistance of a carbon fibre-reinforced polymer (CFRP) composite have been investigated under quasi-static and low velocity impact loading conditions. The perforation data have been supplemented with results from additional flexural tests on scaled composite beams, which highlighted a decrease in both strength and failure strain as scale size increases. Strain-rate effects in this composite have been also identified, with the plates absorbing less energy as the loading-rate is increased. Tests on scaled plates have shown that the normalised perforation energy increases rapidly with scale size. An examination of the load-displacement response indicates that the elastic response obeys a simple scaling law, whereas that the damage does not. It was found that fibre damage was more severe in larger composite panels. It is argued that the energy absorbed in fibre fracture does not scale in the expected manner, leading to greater levels of fibre damage in the larger plates.

.

Keywords: Scaling effects; Perforation resistance; Low-velocity impact; CFRP laminates

1. Introduction

As a result of the attractive range of properties that they offer, fibre-reinforced polymer (FRP) composites have been increasingly used to manufacture large load-bearing structures in the aerospace and marine industries. The use of these lightweight materials often necessitates extensive testing on full-scale prototypes to ensure that structures based on these systems achieve the required performance. Frequently, by applying the principles of similitude (i.e. dimensional analysis), such validation is conducted on small-scale models or based on the results obtained by testing small-scale laboratory specimens to save time and financial costs. However, a concern arising from the use of small-scale models or laboratory specimen

testing for validation is that the mechanical behaviour or response often does not truly represent that of the full-scale structure, due to a number of reasons, including the fact that there is an increased possibility of defects leading to a reduced strength in the actual structural components [1, 2]. Therefore, to successfully design a composite structure or component, it is important to identify scaling effects in the mechanical response, to ensure that the behaviour of the full-scale structure can be predicted by extrapolating from that of the small-scale model.

Initial research on this topic focused on investigating scaling effects in the material strength of unnotched composites [2-7]. Kellas *et al* [4, 5] investigated scaling effects in unidirectional carbon fibre-reinforced plastic (CFRP) laminates using the Buckingham-Π theorem [8], observing significant scaling effects in both the tensile strength and flexural strength of the laminates. Wisnom [7] conducted a number of bending and buckling tests on CFRP laminates, where it was shown that the bending and compressive strengths of the specimens tended to decrease with an increase in specimen size. Given that composite structures are very sensitive to the presence of notches, which are primary sites of stress concentration and damage initiation, attention has focused on investigating scaling effects in the notched strength of composites [9-14]. For example, Wisnom and co-workers [9, 10] performed scaled tests on open-hole composite specimens and highlighted scaling effects in the notched strength, with failure mechanisms including fibre failure and delamination showing a dependence on specimen size.

There has been a growing interest in understanding scaling effects in the impact response of composites as load-bearing composites are increasingly exposed to dynamic loading conditions. In an experimental study performed by Morton [15], size effects in the impact response of some unidirectional CFRP laminates with different stacking sequences were investigated using the Buckingham-Π theorem [8]. It was noted that the impact force should scale as the scaling factor squared, while the impact contact time should scale linearly with the scaling factor. It was observed that the laminate strength increased significantly with decreasing specimen size. Swanson [16] performed drop-weight and airgun impact tests on CFRP plates and cylinders. It was found that the severity of delamination depended on specimen size, whereas the strength and failure strain of the composites did not vary greatly with specimen size. Detailed studies have also been performed to investigate scaling effects in both the quasi-static and low-velocity impact responses of fibre-metal composites and rigid-foam core/CFRP skin sandwich structures [17-19]. It was shown that for both types of material, there was no significant scaling effect in the mechanical

response under quasi-static loading conditions. Similarly, under impact, the contact force, deflection and damage threshold energy were found to be independent of size.

An examination of the published research on scaling effects in composites indicates that most of the existing studies have focused on investigating the response of the laminates based on unidirectional composites, while little attention has been given to woven and textile composites, despite the fact that these materials offer many advantages, such as an improved notched sensitivity, a superior impact resistance, an enhanced drapability, as well as lower fabrication costs, compared to their unidirectional counterparts. It is also evident that very little work has been undertaken at energies above that required for the projectile to perforate the composite target. This threshold is clearly of importance when designing structures and components that are required to protect personnel during dynamic events such as blast and explosions. The aim of this work is therefore, to investigate experimentally scaling effects in the perforation resistance of plain woven CFRP laminates under both quasi-static and low-velocity impact loading conditions.

2. Similitude approach

The similitude approach, applied to the scale-model testing, defines a geometrically-similar scaling law that can be utilised to predict the response parameters of a specimen from a set of appropriately-selected input parameters. The input parameters include both geometrical and material parameters. The geometrical input parameters consist of a length term, L, a width term, W, and a thickness term, h, characterising the overall sizes of each scaled specimen. The material input parameters typically include the elastic properties (e.g. Young's modulus) and the density of the material under consideration. Additional input parameters, such as the loading velocity, the diameter of the impactor or indentor and the size of the support are also defined. The response parameters, i.e. the output parameters or the parameters of interest, generally include the central deflection of the specimen, the measured contact load, the impact duration and the load-deflection response. The dimensions of these parameters are summarised in Table 1, where the requirements for accurate scale modelling of each parameter with respect to the scaling factor, n, which is the ratio of a characteristic length in the scale model to that in the full-scale structure, have been defined. When performing impact scaling tests of the nature, it must be ensured that the impact mass scale as n^3, whereas the impact velocity remains constant in all tests.

3. Experimental procedure

3.1 Test material and specimen configurations

The specimens used in this investigation were fabricated from prepreg sheets of EP121-C15-53 composite material [20]. This particular system, supplied by Gurit Ltd, consists of a 3k HTA plain woven carbon fibre fabric pre-impregnated with 53% EP121 epoxy resin. The fabric has an areal density of 193 g/m^2 (±5%) and the epoxy resin is a highly-toughened, self-extinguishing system that can be cured at temperatures between 120 and 160 °C. In its as-supplied form, the prepreg has a nominal thickness of 0.28 mm and a fibre volume fraction of approximately 39%. All the laminates were prepared by a hand lay-up technique at room temperature and cured using a hot-press at a constant pressure of 2 bar with a dwell temperature of 135° for 70 minutes, before cooling slowly to room temperature. Four scaled sizes of specimen, henceforth referred to as 1/4, 1/2, 3/4 and 1 (full scale), were fabricated, based on 4, 8, 12 and 16 layers of the prepreg respectively, as shown in Figure 1.

3.2 Flexural tests

Potential scaling effects in the perforation response of the composite laminates were explained, in part by conducting scaled three-point bend tests on four scaled sizes of beam, the dimensions of which are given in Table 2. Quasi-static tests were performed on an Instron universal testing machine using a load cell with a maximum capacity of 100 kN. The scaled beams were placed on two cylinders, attached to two adjustable steel supports, and transversely loaded at their centres by a steel cylinder at a crosshead displacement rate of $V = 4n$ mm/min, as shown in Figure 2a. During the test, the force and crosshead displacement were recorded for later analysis. The tests were interrupted when the composite beam had fractured. In order to satisfy the requirements for scaling, the diameters of the support pins and the loading nose used were set to $20n$ mm, and the distance between the two supports was set to $200n$ mm, as summarised in Table 3.

Scaling effects in the impact response of the composite beams were investigated using an instrumented drop-weight test set-up. The dimensions of the supports and loading cylinder for the impact flexural tests were the same as those of the quasi-static flexural tests, Table 3. The release height for all of the scaled impact tests was fixed at 500 mm, giving a constant impact velocity of approximately 3.13 m/s. The mass of the impactor was $14.72n^3$ kg, yielding an impact energy of $72.12n^3$ Joules. This value of energy was just greater than that required to fracture the composite beams. A Kistler 9021A piezo-electric load cell, with a maximum capacity of 10 kN, was used to record the load-time history. A high-speed

camera was positioned in front of the tower to capture the movement of the carriage and the deformation of the specimen during the impact event. The resulting images were analysed using the motion analysis software ProAnalyst in order to obtain the displacement-time history, and subsequently combined with the load-time history to establish the load-displacement history.

3.3 Perforation tests

Quasi-static perforation tests were also conducted on the samples, as outlined in Table 2. In each test case, the square panel was placed on a steel support ring with an inner diameter of $200n$ mm and loaded at the centre by a hemispherical indentor with a diameter of $20n$ mm, as illustrated in Figure 2b. The tests were performed on the aforementioned Instron universal test machine at a constant crosshead displacement rate of $\mathrm{V} = 4n$ mm/min and terminated when a crosshead displacement of $40n$ mm was reached, to ensure that the composite panel was fully perforated. The test conditions for these scaling tests are summarised in Table 4. In order to compare the responses of the composite under conditions below those required for perforation, an additional series of quasi-static tests was undertaken, in which individual tests were stopped at crosshead displacements of either $16n$ or $24n$ mm. These crosshead displacements were selected to ensure that the composite panels exhibited some level of intermediate damage, without being fully perforated.

Scaling effects in the impact perforation response of the composite laminates were also conducted using the instrumental drop-weight test set-up. The dimensions of the support rings and indentors used in the impact perforation tests were the same as those employed for the quasi-static perforation tests, Table 4. Again, the release height for all tests was 500 mm (impact velocity = 3.13 m/s). The impact mass was $34.84n^3$ kg, giving an impact energy of $170.7n^3$ Joules. After testing, the total crack length on the lower surface of each panel was measured and recorded. In addition, a number of samples were sectioned and photographed in order to highlight the failure mechanisms.

Following the quasi-static and dynamic perforation tests, it was found that the composite exhibited some degree of strain-rate dependence. To further investigate such effects, additional perforation tests were conducted on five-ply composite panels with dimensions of 130 × 130 × 1.4 mm. During these tests, the specimens were placed on the $n = 1/2$ support ring and perforated using the $n = 1/2$ impactor at crosshead displacement rates of 0.1, 1, 10, 100 and 188,000 mm/min (3.13 m/s) respectively. Tests up to 100 mm/min were carried out on the Instron test machine, whereas the test at the highest rate was conducted using the drop-weight tower.

4. Results and discussion

4.1 Scaling effects in the flexural response

Figures 3a and 3b show the load-displacement traces obtained following the quasi-static and impact flexural tests respectively. The quasi-static load-displacement traces exhibit similar trends, with the load increasing almost linearly to a maximum, followed by a sharp drop to zero. There is a small decrease in stiffness when the load approaches the maximum value, which is believed to be associated with the presence of localised fibre fracture close to the centre of the beam. A subsequent inspection of the beams indicated that they failed largely as a result of localised fibre fracture at their centres, as shown in Figure 4. No obvious delamination was observed in any sample. The impact load-displacement traces exhibit similar trends to those observed following quasi-static testing, except for the presence of pronounced oscillations up to the maximum force value. Again, the dominant failure mode was fibre fracture in the centre of the beams, similar to that shown for the quasi-static samples in Figure 4.

Scaling effects in the quasi-static and impact flexural responses were investigated by normalising the load data by the square of the scaling factor, n^2 , and the displacement by the scaling factor, n, resulting in Figures 5a and 5b respectively. An examination of the two figures suggests that the scaled load-displacement traces for both the quasi-static (Figure 5a) and impact cases (Figure 5b) appear to collapse onto a single curve, suggesting that the flexural stiffness of this type of composite laminates obeys a simple scaling law, indicating that the flexural modulus of this composite is independent of specimen size. In contrast, the scaled maximum force shows a notable dependence on geometry, decreasing with increasing scale size, with the reduction over the range of scale sizes being 19 % for the quasi-static samples and 14 % for the impact specimens. Similar size effects are seen in the scaled displacements at failure. Such a pronounced size dependence in the scaled maximum load and the scaled displacement at failure clearly indicate that the flexural strength and failure strain of this composite do not scale. Figure 5b shows that the impact-loaded beams exhibit a higher stiffness and a lower failure strain, relative to their quasi-static counterparts. It is believed that the higher stiffness under impact loading condition is associated with the weave having less time to deform and flatten at high strain-rates. Another consequence is that the damage initiation and propagation in the composite during the impact event may be postponed, leading to a higher material strength.

The size independence of the flexural modulus and size dependency of the flexural strength and failure strain, can be accounted for by the following two facts. On one hand, the flexural modulus of a woven composite laminate is a volume-averaged quantity, being determined by the volume fractions of the polymer matrix and woven fabric and by the presence of micro-defects (e.g. microvoids). Since the volume fractions of the material constituents and micro-defects in the laminates are statistically constant and do not vary with specimen size, volume-averaged quantities such as the flexural modulus should also be independent of scale size. On the other hand, the flexural strength of the composite laminate is not a volume-averaged quantity since failure tends to initiate from stress concentrations, such as local defects and microvoids, in the highly-stressed region of the beam. Consequently, larger composite beams, which have greater numbers of defects in the highly-stressed regions, tend to fail at lower strength values.

4.2 Strain-rate effects in the perforation resistance

The load-displacement traces following perforation tests at different crosshead displacement rates on the five-ply composite panels are shown in Figure 6a. Here, it is evident that the curves exhibit similar trends, with the load gradually increasing to a maximum value before tending to plateau, after which the load decreases dramatically to another plateau, associated with frictional effects as the hemispherical indentor passes through the panel. The underlying failure mechanisms associated with the presence of the former plateau in the load-displacement curves will be addressed in the next section. It is interesting to note that the initial stiffness and maximum load increase with the crosshead displacement rate, whereas the displacement at failure (defined at the onset of the lowermost plateau) decreases. Again, as discussed previously, the increases in the maximum load and stiffness are likely to be associated with the fact that a higher loading rate gives the composite less time to deform, postponing damage initiation and propagation in the composite. Similar strain-rate effects in the stiffness of woven CFRP composites have also been observed following impact bending tests in the study outlined by Ullah *et al* [21]. Figure 6b shows the variation of the total absorbed energy with crosshead displacement rate, where it is evident that the perforation energy decreases by almost 20% over the range of strain-rates considered.

4.3 Scaling effects in the perforation response

Prior to investigating the perforation response of the laminates, a series of quasi-static tests were undertaken on scaled plates in which the tests were terminated at crosshead displacements of $16n$ and $24n$ mm. These tests were conducted in order to assess the level of damage at each of these scaled displacements and to investigate the reproducibility of the various parts of the load-displacement trace.

Figure 7 shows the load-displacement traces for two of these cases (n=1/4 and n=1) in which the complete perforation trace (crosshead displacement of 40n mm is included). An examination of the figures indicates that there is an excellent repeatability for each scale size, with the 16n and 24n mm traces mapping exactly onto the 40n mm case. The severity of damage was characterised by measuring the length of the rear surface fibre fracture and then normalising by twice the panel width (since cracks extended in the warp and weft directions), and the resulting data for the interrupted tests are shown in Figure 8. It is clear that the normalised length of fibre fracture increases rapidly with scale size for a given crosshead displacement. For example, the normalised crack length increases by 300 % across the range of scale sizes for a crosshead displacement of 24n mm.

Figures 9a and 9b show the load-displacement traces obtained following quasi-static and impact tests on the four scaled sizes of specimen. Here, both sets of load-displacement traces show similar features to those observed following tests on the 5-ply laminates, with the load increasing to a maximum before plateauing at an approximately constant force, after which, the load drops rapidly to second plateau, associated with frictional effects between the indentor and the plate. A subsequent examination of the perforated specimens highlighted that the presence of fibre fracture extending from the centre of the panel in both the warp and weft directions as well as delamination. Figures 10 and 11 show cross-sections of the perforated panels following testing at quasi-static and impact rates of strain, respectively. An examination of Figure 10 suggests that the failure mechanisms are similar at all scale sizes, with fibre fracture being predominant in all cases. Under impact loading conditions, there is evidence of limited delamination in the two larger scale sizes. In spite of this, it is surprising to see how similar the perforation zones are in the four scaled sizes. Clearly, the photos of the cross-sections of the perforated panels were taken after removing the projectile. The removal of the projectile reduced the width of the crack that was formed during the perforation event, as a consequence of the elastic springback of the panel. It is therefore somewhat difficult to observe the prevailing failure mechanisms from the cross-sections of these panels. For clarity, a photo showing the rear view of a perforated panel following quasi-static perforation is shown in Figure 10e and that for the case of impact perforation in Figure 11e. It is believed that the maximum force observed in the load-displacement curves in Figure 9 coincides with the onset of lower surface fibre fracture and that the subsequent plateau in the force-displacement curve is associated with fibre fracture extending away from the centre of the panel. Furthermore, the lower non-zero plateau value of force in the load-displacement curve is again a result of friction between the impactor and the panel.

The load-displacement traces in Figures 9a and 9b were normalised using the procedures outlined above and the results for the quasi-static and impact tests are shown in Figures 12a and 12b, respectively. For both strain-rates, the initial elastic portions coincide, indicating once again that the elastic response of this composite obeys a simple scaling law. However, the maximum load tends to decrease with increasing scale size, particularly in the quasi-static samples, suggesting that the strength of this composite decreases with scale size. Similar trends were observed under flexural loading and this was associated with the presence of a greater number of defects in the highly-stressed region under the indentor, as discussed previously in Section 4.1. Such trends in the maximum strength are not apparent under impact loading, although they may be masked by the highly oscillatory trends in the experimental curves. In addition, the length of the force plateau increases significantly with increasing scale size.

In order to quantify the severity of damage in the perforated panels, the total crack length on the rear surface was measured and then normalised, as before, by dividing this value by twice the panel edge length. The resulting data are presented in Figure 13a. The figure clearly shows that under both quasi-static and impact perforation conditions, damage in these laminates does not obey a scaling law, since it becomes more severe as scale size is increased. For example, at quasi-static rates, the normalised damage in the full-scale panel was approximately twice that in the smallest panel. Under impact conditions damage was approximately three times of that in the ¼ panel. The increased severity of damage in larger composite panels can be explained partly as a result of the lower flexural strength in the larger samples (Figure 5b) and also from an energy point of view, as follows. The amount of energy required to create fibre fracture is jointly determined by the total area of fracture that is created and the fracture energy associated with this failure mode. It should be noted that the physical widths of the cracks in the warp and weft directions were similar in all scaled sizes of specimen as the cracks were constrained by adjacent tows and could not propagate laterally. The energy associated with fibre fracture can be therefore estimated from:

$$\mathrm{E}_f = hl\gamma$$

where γ denotes the fracture energy associated with this fibre-dominated failure mode, i.e. fibre fracture, and h and l represent the thickness of specimen and the length of fibre fracture, respectively. As γ is an intrinsic material property and independent of scale size, this energy term scales as n^2, rather than n^3, as is the case for the input energy. During the perforation event, the elastic energy absorbing capability (a parameter that scales as n^3) of this composite laminates has been surpassed, an additional amount of

energy must be absorbed in failure mechanisms, primarily through further propagation of fibre fracture, since matrix damage and delamination in this highly-toughened epoxy resin composites is relatively small, as observed in all perforated panels. Given that the energy absorbed in the fibre fracture process and the incident energy scale differently, it is argued that larger areas of fibre fracture are required to absorb the 'additional' amount of energy associated with perforation on larger specimens.

The evidence presented in Figure 13a clearly demonstrates that perforation damage in these laminates does not obey a simple scaling law, with damage becoming more severe with an increase in scale size. The energy absorbed during the perforation event for each scale size and loading condition was calculated as the area under the load-displacement trace, and the variation of this energy with scale size is shown in Figure 13b. Although there is some scatter in the trends in the energies associated with the intermediate scale sizes under impact loading, the data suggest that at both strain-rates, the absorbed energy increases with scale size. Looking at the scaled load-displacement traces in Figure 12, it is clear that the extended regions associated with the fibre fracture phases in the larger samples lead to a significant increase in the maximum displacement and greater energy absorption, as evidenced by the area under the traces.

It is worth noting that the damage in the perforated quasi-static panels was more severe than in the impact perforated panels, as shown in Figures 13a and 13b, where it is evident that for each scale size, both the normalised crack length and the scaled absorbed energy under quasi-static loading are significantly greater than those associated with impact loading. This effect can be partly explained from the data on the 5-ply laminates, where it was noted that the panel was stiffer at higher rates of loading, which is again confirmed from the combined scaled load-displacement traces, as shown in Figure 12b.

5. Conclusions

Scaling effects in the perforation resistance of plain woven CFRP composite laminates have been investigated under both quasi-static and impact loading conditions. Trends in the experimental results have been explained using additional data generated through a series of flexural tests on scaled beams. It has been shown that the elastic response of the composite beams and plates follows a scaling law, whereas the maximum load at failure generally decreases with increasing scale size. It is believed that the decrease in strength in the larger composite samples is associated with an increased presence of defects in the highly-stressed regions of the structure.

Perforation tests over a wide range of strain-rates have highlighted a pronounced rate-sensitivity, with the energy required to perforate the laminates decreasing with increasing crosshead displacement rate. It has been shown that the perforation resistance of the woven CFRP panels does not scale, with the energy absorbed during perforation increasing rapidly with scale size. Similarly, the observed damage does not scale in accordance with that predicted by simple scaling laws. A subsequent examination of the perforated composite panels confirmed that fibre damage, in the form of large cracks propagating in the warp and weft directions, was more severe in larger composite panels. It is argued that under impact, for example, the energy absorbed in fibre fracture scales with the square of the scaling factor, i.e. n^2, whereas the incident energy scales as n^3. This discrepancy results in increased levels of energy being absorbed in fibre fracture mechanisms and greater damage in the larger panels.

Acknowledgements.

The lead author, Z.W. Xu, gratefully acknowledges the financial support from the China Scholarship Council (CSC) under grant number 201408060025.

References.

[1] L. S. Sutherland, R. A. Shenoi, and S. M. Lewisc, "Size and scale effects in composites: I. Literature review," *Composites Science and Technology,* vol. 59, pp. 209-220, 1999.

[2] M. R. Wisnom, "Scaling effects in the testing of fibre-composite materials," *Composites Science and Technology,* vol. 59, pp. 1937-1957, 1999.

[3] K. E. Jackson, "Scaling effects in the flexural response and failure of composite beams," *AIAA Journal,* vol. 30, pp. 2099-2105, 1992.

[4] K. E. Jackson, S. Kellas, and J. Morton, "Scale Effects in the Response and Failure of Fiber Reinforced Composite Laminates Loaded in Tension and in Flexure," *Journal of Composite Materials,* vol. 26, pp. 2674-2705, 1992.

[5] S. Kellas and J. Morton, "Strength scaling in fiber composites," *AIAA Journal,* vol. 30, pp. 1074-1080, 1992.

[6] D. P. Johnson, J. Morton, S. Kellas, and K. E. Jackson, "Size Effects in Scaled Fiber Composites Under Four-Point Flexure Loading," *AIAA Journal,* vol. 38, pp. 1047-1054, 2000.

[7] M. R. Wisnom, "The effect of specimen size on the bending strength of unidirectional carbon fibre-epoxy," *Composite Structures,* vol. 18, pp. 47-63, 1991.

[8] E. Buckingham, "On Physically Similar Systems; Illustrations of the Use of Dimensional Equations," *Physics Reviews,* vol. 4, pp. 345-376, 1914.

[9] B. G. Green, M. R. Wisnom, and S. R. Hallett, "An experimental investigation into the tensile strength scaling of notched composites," *Composites Part A: Applied Science and Manufacturing,* vol. 38, pp. 867-878, 2007.

[10] M. R. Wisnom, S. R. Hallett, and C. Soutis, "Scaling Effects in Notched Composites," *Journal of Composite Materials,* vol. 44, pp. 195-210, 2009.

[11] G. H. Erçin, P. P. Camanho, J. Xavier, G. Catalanotti, S. Mahdi, and P. Linde, "Size effects on the tensile and compressive failure of notched composite laminates," *Composite Structures,* vol. 96, pp. 736-744, 2013.

[12] X. Xu, M. R. Wisnom, X. Li, and S. R. Hallett, "A numerical investigation into size effects in centre-notched quasi-isotropic carbon/epoxy laminates," *Composites Science and Technology,* vol. 111, pp. 32-39, 2015.

[13] J. Serra, C. Bouvet, B. Castanié, and C. Petiot, "Scaling effect in notched composites: The Discrete Ply Model approach," *Composite Structures,* vol. 148, pp. 127-143, 2016.

[14] K. Tang, H. Bao, and G. Liu, "Simulation on size effect of notched quasi-isotropic composite laminates under tensile loading," *Journal of Reinforced Plastics and Composites,* vol. 35, pp. 1623-1633, 2016.

[15] J. Morton, "Scaling of impact-loaded carbon-fiber composites," *AIAA Journal,* vol. 26, pp. 989-994, 1988.

[16] S. R. Swanson, "Scaling of impact damage in fiber composites from laboratory specimens to structures," *Composite Structures Volume,* vol. 25, pp. 249-255, 1993.

[17] J. G. Carrillo and W. J. Cantwell, "Scaling Effects in the Low Velocity Impact Response of Fiber-Metal Laminates," *Journal of Reinforced Plastics and Composites,* vol. 27, pp. 893-907, 2008.

[18] S. McKown, W. J. Cantwell, and N. Jones, "Investigation of Scaling Effects in Fiber--Metal Laminates," *Journal of Composite Materials,* vol. 42, pp. 865-888, 2008.

[19] F. J. Yang, M. Z. Hassan, W. J. Cantwell, and N. Jones, "Scaling effects in the low velocity impact response of sandwich structures," *Composite Structures,* vol. 99, pp. 97-104, 2013.

[20] Gurit. (2017). *DATASHEET / EP 121 - Epoxy Prepreg* Available: http://www.gurit.com/-/media/Gurit/Datasheets/ep-121pdf.ashx

[21] H. Ullah, A.R. Harland, and V. V. Silberschmidt, "Dynamic bending behaviour of woven composites for sports products: experiments and damage analysis," *Materials & Degsign,* vol. 88, pp. 149-156, 2015.

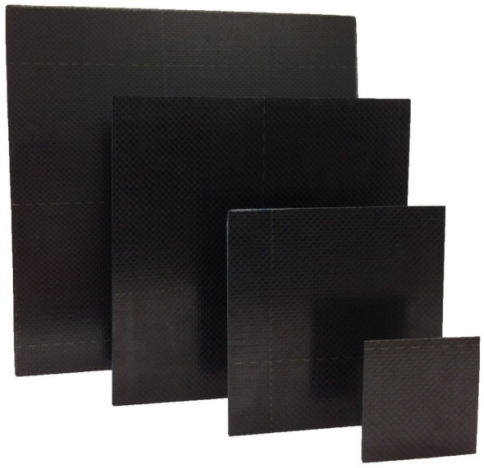

Figure 1. Photos of the four scaled sizes of perforation panel.

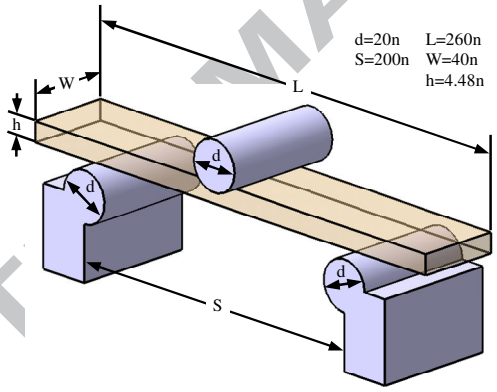

(a) Schematic of the scaled flexural tests.

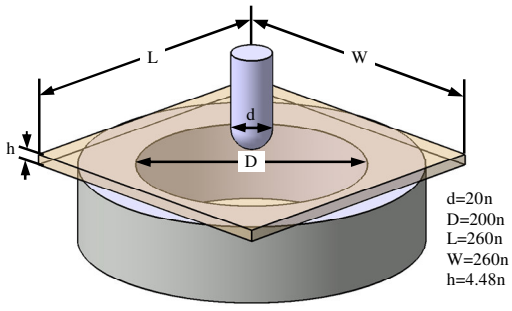

(b) Schematic of the scaled perforation tests.

Figure 2. Schematics of the flexural and perforation tests

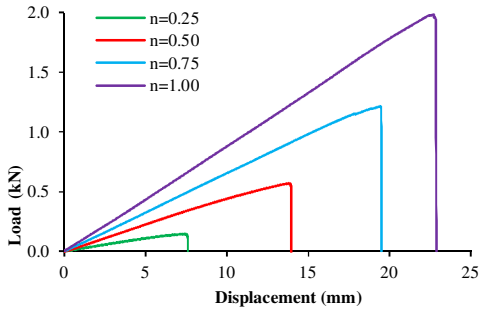

(a) Traces following quasi-static flexural tests.

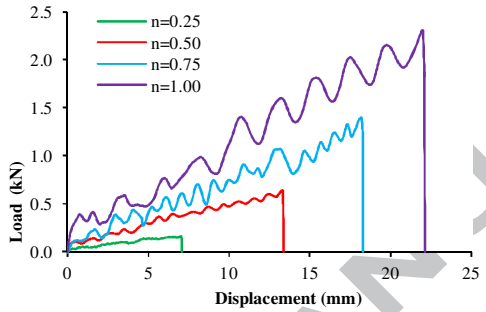

(b) Traces following impact flexural tests.

Figure 3. Load-displacement traces following flexural testing.

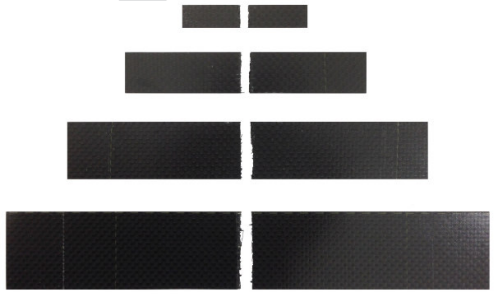

Figure 4. Fractured samples following quasi-static flexural testing.

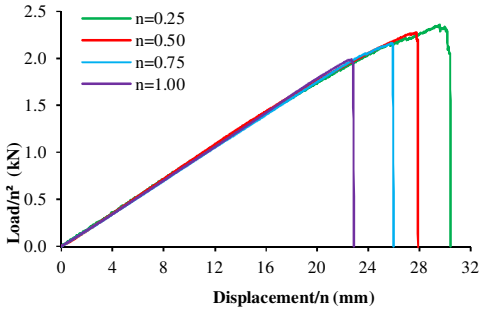

(a) Scaled traces following quasi-static flexural testing.

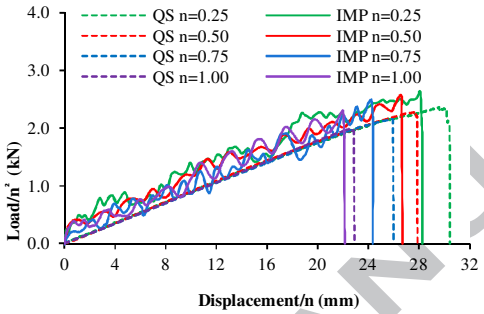

(b) Scaled traces following impact (IMP) flexural testing. The quasi-static (QS) traces are included for comparison.

Figure 5. Scaled load-displacement traces following flexural testing.

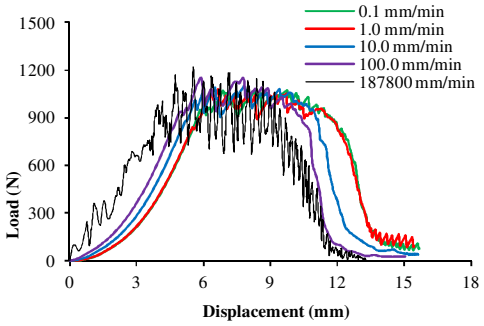

(a) Influence of crosshead displacement rate on the perforation response.

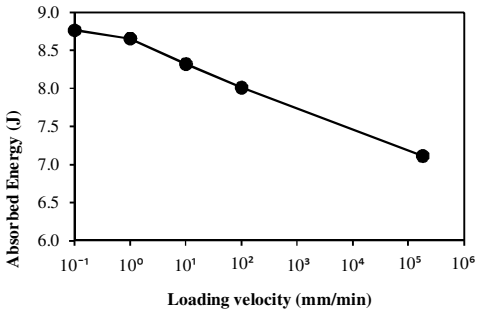

(b) The variation of perforation energy with crosshead displacement rate.

Figure 6. (a) Load-displacement traces at different crosshead displacement rates and (b) the resulting absorbed energies following perforation tests on the 5-ply laminates.

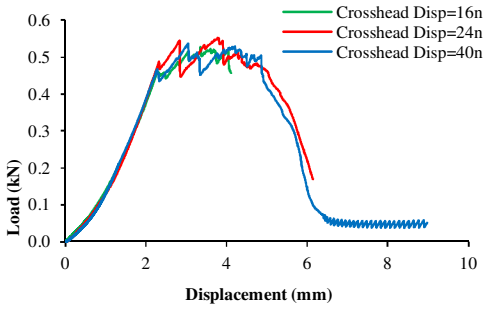

(a) Scale size n=0.25

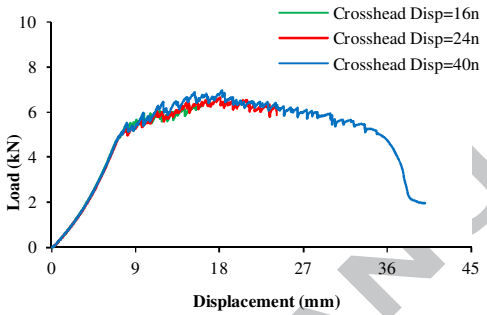

(b) Scale size n=1

Figure 7. Load-displacement traces for the quasi-static perforation tests under the total crosshead displacements of $16n$, $24n$ and $40n$

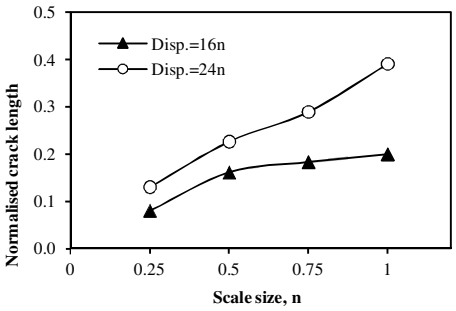

Figure 8. Scaled crack lengths following quasi-static indentation tests up to normalised crosshead displacements of $16n$ and $24n$ mm.

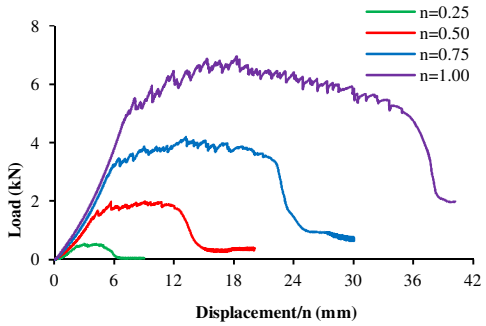

(a) Load-displacement traces following quasi-static perforation tests to a crosshead displacement of 40*n* mm.

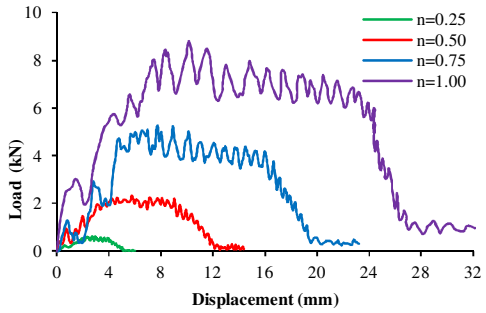

(b) Load-displacement traces following impact perforation tests.

Figure 9. Load-displacement traces following quasi-static and impact perforation tests.

(a) n=0.25

(b) n=0.5

(c) n=0.75

(d) n=1

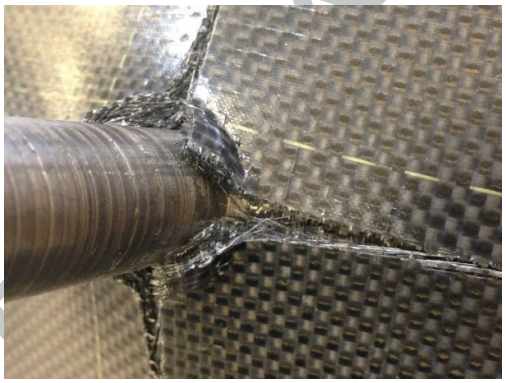

(e) Rear view of a perforated panel with the projectile remaining in place.

Figure 10. Cross-sections and a rear view of perforated panels following quasi-static testing.

(a) n=0.25

(b) n=0.5

(c) n=0.75

(d) n=1

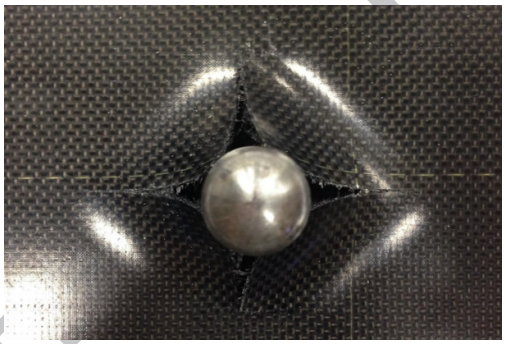

(e) Rear view of a perforated panel with the projectile remaining in place.

Figure11. Cross-sections and a rear view of panels following impact perforation tests.

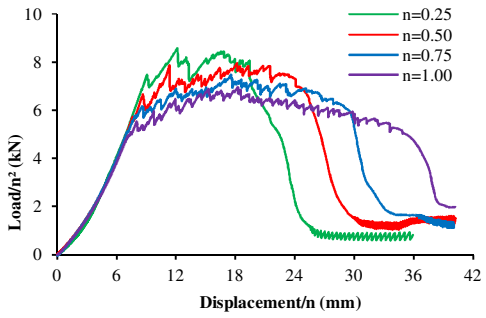

(a) Scaled load-displacement traces following quasi-static perforation tests.

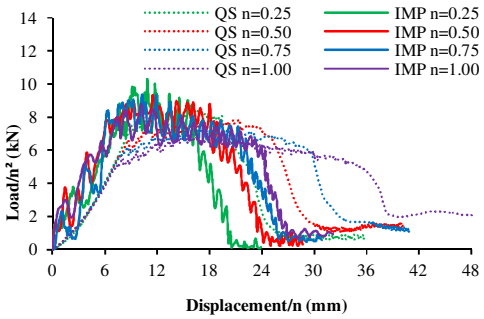

(b) Scaled load-displacement traces following impact (IMP) perforation tests. The quasi-static (QS) traces are included for comparison.

Figure 12. Scaled load-displacement traces following quasi-static and impact perforation tests.

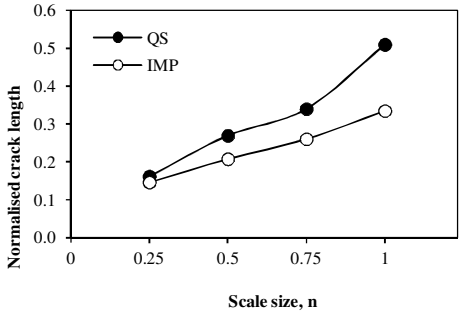

(a) Normalised crack length versus scale size following quasi-static (QS) and impact (IMP) perforation tests.

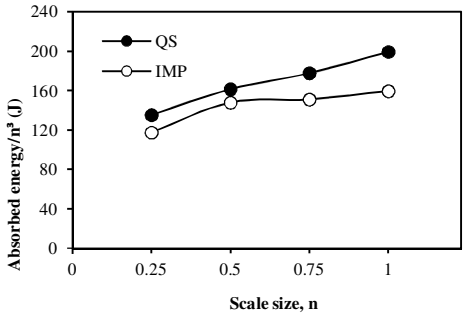

(b) Scaled absorbed energy versus scale size following quasi-static (QS) and impact (IMP) perforation tests.

Figure 13. The variation of (a) the normalised crack length and (b) the normalised absorbed energy with scale size following quasi-static and impact perforation tests.

Table 1. Summary of scale model parameters and their dependencies on the scaling factor.

Parameter	Scaling factor
Specimen length	n
Specimen width	n
Specimen thickness	n
Diameter of loading cylinder *	n
Diameter of indentor **	n
Support span *	n
Support ring size **	n
Impact mass	n^3
Impact energy	n^3
Maximum impact force	n^2
Target displacement	n

* for flexural tests

** for perforation tests

Table 2. Geometrical configurations of the specimens used in flexural and perforation tests

Scale n	Length (mm)	Plate width* (Beam)	Thickness (mm)	No. of plies
1/4	65	65 (10)	1.12	4
1/2	130	130 (20)	2.24	8
3/4	195	195 (30)	3.36	12
1	260	260 (40)	4.48	16

* for perforation tests

** for flexural tests

Table 3. Summary of the test conditions for quasi-static and impact flexural tests

Scale n	Loading Cylinder diameter	Support roller diameter	Support span (mm)	Disp. rate (mm/min)*	Drop height (mm)**
1/4	5	5	50	1	500
1/2	10	10	100	2	500
3/4	15	15	150	3	500
1	20	20	200	4	500

* for quasi-static tests

** for impact tests

Table 4. Summary of the test conditions for quasi-static and impact perforation tests.

Scale n	Indentor diameter (mm)	Ring inner diameter (mm)	Crosshead speed*	Drop-height** (mm)	Mass** (kg)
1/4	5	50	1	500	0.54
1/2	10	100	2	500	4.36
3/4	15	150	3	500	14.70
1	20	200	4	500	34.84

* for quasi-static perforation tests

** for impact perforation tests